

THE JOURNAL OF PHYSICAL CHEMISTRY **Caltech** Library

Subscriber access provided by Caltech Library

C: Energy Conversion and Storage; Energy and Charge Transport

Electrolyte-Assisted Hydrogen Storage Reactions

John J. Vajo, Hongjin Tan, Channing C. Ahn, Dan Addison, Son-Jong Hwang, James L. White, Timothy C. Wang, Vitalie Stavila, and Jason Graetz

J. Phys. Chem. C, **Just Accepted Manuscript** • DOI: 10.1021/acs.jpcc.8b08335 • Publication Date (Web): 05 Nov 2018Downloaded from <http://pubs.acs.org> on November 6, 2018

Just Accepted

“Just Accepted” manuscripts have been peer-reviewed and accepted for publication. They are posted online prior to technical editing, formatting for publication and author proofing. The American Chemical Society provides “Just Accepted” as a service to the research community to expedite the dissemination of scientific material as soon as possible after acceptance. “Just Accepted” manuscripts appear in full in PDF format accompanied by an HTML abstract. “Just Accepted” manuscripts have been fully peer reviewed, but should not be considered the official version of record. They are citable by the Digital Object Identifier (DOI®). “Just Accepted” is an optional service offered to authors. Therefore, the “Just Accepted” Web site may not include all articles that will be published in the journal. After a manuscript is technically edited and formatted, it will be removed from the “Just Accepted” Web site and published as an ASAP article. Note that technical editing may introduce minor changes to the manuscript text and/or graphics which could affect content, and all legal disclaimers and ethical guidelines that apply to the journal pertain. ACS cannot be held responsible for errors or consequences arising from the use of information contained in these “Just Accepted” manuscripts.



ACS Publications

is published by the American Chemical Society, 1155 Sixteenth Street N.W.,
Washington, DC 20036Published by American Chemical Society. Copyright © American Chemical Society.
However, no copyright claim is made to original U.S. Government works, or works
produced by employees of any Commonwealth realm Crown government in the course
of their duties.

Electrolyte-Assisted Hydrogen Storage Reactions

John J. Vajo^{1}, Hongjin Tan^{2**}, Channing C. Ahn^{2,3}, Dan Addison², Son-Jong Hwang⁴,*

James L. White⁵, Timothy C. Wang⁵, Vitalie Stavila⁵, Jason Graetz¹

1) HRL Laboratories, LLC, 3011 Malibu Canyon Road, Malibu, CA 90265

2) Liox Power, Inc., 129 North Hill Ave., Suite 107, Pasadena, CA 91106

3) Division of Engineering and Applied Science, California Institute of Technology,

Pasadena, CA 91125

4) Division of Chemistry and Chemical Engineering, California Institute of Technology,

Pasadena, CA 91125

5) Sandia National Laboratories, P.O. Box 969, Livermore, CA, 94551

1
2
3
4 **Corresponding Author**
5

6
7 * jjvajo@hrl.com
8
9

10
11
12
13
14
15
16
17
18
19 **Abstract**
20

21
22
23 Use of electrolytes, in the form of $\text{LiBH}_4/\text{KBH}_4$ and LiI/KI/CsI eutectics, is shown to
24
25
26 significantly improve (by more than a factor of ten) both the dehydrogenation and full
27
28
29 rehydrogenation of the MgH_2/Sn destabilized hydride system and the hydrogenation of
30
31
32 MgB_2 to $\text{Mg}(\text{BH}_4)_2$. The improvement revealed that inter-particle transport of atoms
33
34
35
36
37 heavier than hydrogen can be an important rate-limiting step during hydrogen cycling in
38
39
40
41 hydrogen storage materials consisting of multiple phases in powder form. Electrolytes
42
43
44 enable solubilizing heavy ions into a liquid environment and thereby facilitate the reaction
45
46
47
48 over full surface areas of interacting particles. The examples presented suggest that use
49
50
51
52
53
54
55
56
57
58
59
60 of electrolytes in the form of eutectics, ionic liquids, or solvents containing dissolved salts

1
2
3
4 may be generally applicable for increasing reaction rates in complex and destabilized
5
6
7 hydride materials.
8
9
10
11
12
13
14
15
16
17
18
19
20
21
22
23
24
25
26
27
28
29
30
31
32
33
34
35
36
37
38
39
40
41
42
43

44 **Introduction**

45
46
47
48 Hydrogen cycling in high capacity hydrogen storage materials often involves multiple solid
49
50
51 phases in powder-particle form that must interact, nucleate, grow, and shrink during
52
53
54 reaction. These materials, including many complex hydrides¹⁻³ and destabilized hydride
55
56
57
58
59
60

1
2
3 mixtures⁴ (also called reactive hydride composites⁵), have rates of hydrogen uptake and
4
5
6
7 release that are typically very slow. To address this issue, catalytic additives⁶ and
8
9
10 nanoscale formulations⁷⁻⁹ have been studied extensively. These approaches have
11
12
13
14 produced considerable improvements, although the rates of hydrogen cycling are still
15
16
17 typically too limited for practical applications, such as vehicular hydrogen storage. One
18
19
20
21 reason for this limitation may be that both catalytic additives and nanoscale formulations
22
23
24 predominately address atomic transport and reaction within individual particles. However,
25
26
27
28 in multiple solid-phase materials, atomic transport between particles of different phases
29
30
31 is required. This requirement could impose additional kinetic restrictions because inter-
32
33
34
35 particle transport 1) likely involves the motion of atoms heavier than hydrogen, such as
36
37
38 Li, Na, Mg, B, and Al; 2) may occur over relatively long distances (much longer than typical
39
40
41 bond lengths); and 3) can only occur at interfaces where different phase particles come
42
43
44
45 in contact on an atomic scale. For typical powders, this interfacial area may be only a
46
47
48
49 small fraction of the total surface area.
50
51
52
53
54
55
56
57
58
59
60

1
2
3 Here we explore the idea that the kinetics of hydrogen cycling in multiple-phase
4
5
6
7 hydrogen storage materials may be improved through the addition of a liquid electrolyte.
8
9
10 The electrolyte may assist inter-particle transport and promote the overall reaction
11
12
13 (addressing the restrictions listed above) by 1) solubilizing reacting ions; 2) providing
14
15
16
17 liquid-state diffusion rates facilitating long distance transport; and 3) giving transported
18
19
20
21 ions access to the full surface area of the reacting phases by surface wetting, effectively
22
23
24 greatly increasing the number of favorable interactions of the reacting species. We show
25
26
27
28 that using electrolytes can significantly increase the rates of dehydrogenation and
29
30
31 hydrogenation, by factors of $\sim 10\times$ or more. This increase clearly identifies the role of
32
33
34
35 inter-particle transport in governing the overall rates and mechanisms of hydrogen
36
37
38
39 exchange and may provide a useful step towards the eventual commercial application of
40
41
42 these materials by enabling cycling under more moderate conditions closer to chemical
43
44
45 equilibrium.
46
47
48
49
50
51

52 Although to our knowledge, this idea has not been explored explicitly, this work builds
53
54
55
56 upon prior studies that have considered systems in which hydrides were dissolved in
57
58
59
60

1
2
3
4 solvents¹⁰⁻¹⁴, solvate-type hydride adducts were formed¹⁵⁻²⁰, and molten phases were
5
6
7 reported to participate in reaction²¹⁻²³.
8
9
10
11
12
13

14 Results

15
16 To illustrate the influence of an electrolyte on hydrogen cycling in multiple phase hydrogen
17 storage materials we describe results for two systems: MgH₂/Sn and Mg(BH₄)₂. The
18
19 MgH₂/Sn system is a prototypical destabilized hydride in which Sn lowers the enthalpy for
20 dehydrogenation through the formation of Mg₂Sn. During dehydrogenation, MgH₂ and
21
22 Sn, typically milled together as powders, interact to release hydrogen and form Mg₂Sn.
23
24 Upon rehydrogenation, hydrogen interacts with Mg₂Sn to reform separate phases of
25
26 MgH₂ and Sn. This reaction²⁴⁻²⁶, and to a greater extent its analog, MgH₂/Si²⁴⁻²⁹, have
27
28 been studied and found to dehydrogenate with the formation of Mg₂Sn (and Mg₂Si),
29
30 although only at temperatures well above predicted equilibrium temperatures.
31
32 Rehydrogenation has not been observed to any significant extent in previous studies.
33
34 Mg(BH₄)₂ is a complex hydride that is potentially practical due to its high theoretical
35
36 hydrogen content of 14.9 wt% H₂ and favorable equilibrium pressure of 1 bar at ~100
37
38
39
40
41
42
43
44
45
46
47
48
49
50
51
52
53
54
55
56
57
58
59
60

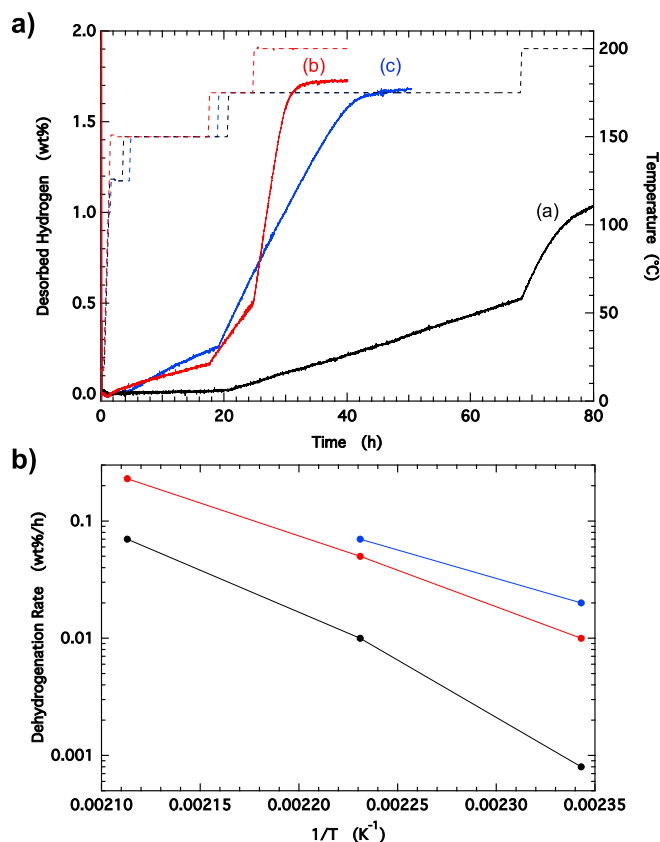
1
2
3 °C.^{30,31} Although initially single phase, its dehydrogenation pathway is complex, with the
4
5
6
7 formation of multiple intermediate phases such as $\text{MgB}_{12}\text{H}_{12}$ and MgH_2 . These phases
8
9
10 must further interact, ultimately forming MgB_2 .³⁰ Significant (>70%) hydrogenation of
11
12
13
14 MgB_2 has been achieved although only under impractical conditions, e.g., ~1000 bar H_2
15
16
17 at ~400 °C.³² Therefore, it is highly desirable to facilitate the rehydrogenation of this
18
19
20
21 system at some more achievable set of conditions.
22
23
24
25
26
27

28 *Electrolyte-assisted hydrogen cycling in MgH_2/Sn .* Dehydrogenation of milled mixtures
29
30
31 of $\text{MgH}_2 + 0.5\text{Sn}$ (theoretical capacity 2.3 wt% H_2) with and without an electrolyte
32
33
34 composed of the eutectic $0.725\text{LiBH}_4/0.275\text{KBH}_4$ are shown in Figure 1. The electrolyte
35
36
37 composition was chosen to minimize the melting point (~110 °C, Figure S1) and to reduce
38
39
40
41 the chance of any side reactions.³³ Samples were prepared by hand-grinding LiBH_4 and
42
43
44
45 KBH_4 , and then adding milled MgH_2/Sn with gentle mixing using a spatula. The mass
46
47
48
49 fraction of hydride in the hydride + electrolyte system was ~50% (increasing the hydride
50
51
52 fraction to practical levels, e.g., >~70%, was not the objective of this work and will be
53
54
55
56 considered elsewhere). The dehydrogenation reactions were conducted under an initial
57
58
59
60

1
2
3 H₂ pressure of 2 bar to prevent any significant direct dehydrogenation of MgH₂ forming
4
5
6
7 Mg metal (the equilibrium temperature for MgH₂ at 2 bar H₂, $T_{\text{eq}}(2 \text{ bar})$, is $\sim 300 \text{ }^\circ\text{C}$). Slow
8
9
10 dehydrogenation was detected at 150 °C (Figure 1a). Without electrolyte, the rate was
11
12
13
14 0.0008 wt% H₂/h. With LiBH₄-KBH₄, the rate (with respect to the MgH₂ + Sn mass only)
15
16
17 increased to 0.010 wt% H₂/h and with LiBH₄-KBH₄ additionally including 0.025MgI₂, the
18
19
20 rate was 0.020 wt% H₂/h. These dehydrogenation reaction rates are 12× and 25× higher,
21
22
23
24 respectively, than the rate without electrolyte. At higher temperatures, smaller increases
25
26
27
28 of 4.7× to 7.3× at 175 °C and 3.2× at 200 °C were observed. Figure 1b depicts the rates
29
30
31 in Arrhenius form. Although there are too few temperatures for accurate estimates, the
32
33
34
35 activation energy does appear to decrease significantly from $\sim 150 \text{ kJ/mol-H}_2$ without
36
37
38 electrolyte to $\sim 100 \text{ kJ/mol-H}_2$ with the 0.725LiBH₄/0.275KBH₄ eutectic. We note that
39
40
41
42 these activation energies are still much higher than the thermodynamic barrier of 39
43
44
45 kJ/mol-H₂, estimated from tabulated thermodynamic data for the pure phases. In addition
46
47
48
49 to increased initial rates with the electrolytes, the dehydrogenation rates remained nearly
50
51
52
53 constant until the reaction was almost complete. In contrast, the rate of reaction without
54
55
56 electrolyte the rate steadily decreases (i.e., at 200 °C, $\sim 70 \text{ h}$, Figure 1), even though the
57
58
59
60

1
2
3 extent of reaction was low. In preliminary similar work, nearly constant dehydrogenation
4
5
6
7 rates were also seen in the MgH_2/Si system (Figure S2). In addition, preliminary
8
9
10 measurements for MgH_2/Sn using several other potential electrolyte systems either
11
12
13
14 appeared to decompose or showed similar or slower rates of dehydrogenation (see SI).
15
16

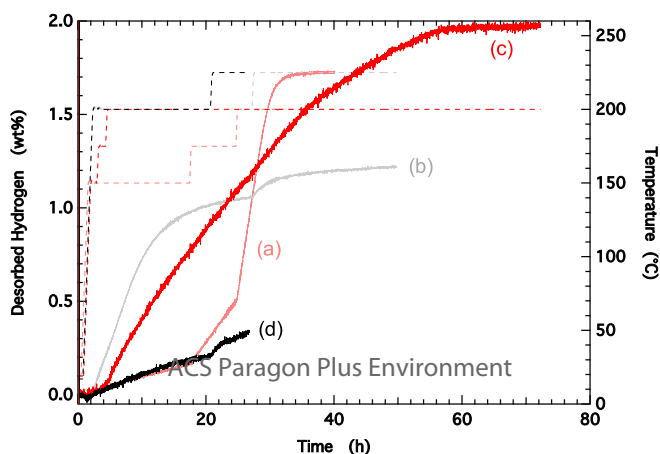
17 **Figure 1.** Dehydrogenation of MgH_2/Sn with and without electrolyte. Panel a) desorbed
18
19
20 hydrogen (curve a, black) without electrolyte; (curve b, red) with added
21
22
23
24



25
26
27
28
29
30
31
32
33
34
35
36
37
38
39
40
41
42
43
44
45
46
47
48
49
50
51 0.725LiBH₄/0.275KBH₄, 50 wt% MgH_2/Sn ; (curve c, blue) with added
52
53
54
55 0.725LiBH₄/0.275KBH₄ + 0.025MgI₂, 44 wt% MgH_2/Sn ; (dashed curves) corresponding
56
57
58
59
60

1
2
3 temperatures, right axis. Panel b) dehydrogenation rates vs. inverse absolute temperature
4
5
6
7 (determined from linear fits to the isothermal intervals; the uncertainties are ~5%, see SI).
8
9
10 Desorbed hydrogen (wt%) and dehydrogenation rates (wt% H₂/h) are with respect to the
11
12
13
14 MgH₂/Sn mass only. Dehydrogenation was conducted in an initial hydrogen pressure of
15
16
17
18 2 bar to suppress direct dehydrogenation of MgH₂ as well as any decomposition of the
19
20
21 electrolyte.
22
23
24
25
26
27

28 To investigate reversibility, samples dehydrogenated with and without LiBH₄-KBH₄
29
30
31 electrolyte were treated in hydrogen at 920 bar to 1000 bar while decreasing the
32
33
34 temperature from 215 °C to 175 °C, over 75 hours (Figure S3). Following this treatment,
35
36
37
38 a second dehydrogenation was conducted. The results are shown in Figure 2. With the
39
40
41 electrolyte, dehydrogenation of ~1.9 wt% occurred indicating nearly complete
42
43
44
45 hydrogenation during the hydrogen treatment. This capacity is ~15% greater than the
46
47
48



1
2
3 capacity for the initial dehydrogenation possibly indicating improved reaction as a result
4
5
6
7 of cycling. Without electrolyte, at most only 0.3 wt% uptake occurred. We consider this
8
9
10 capacity an upper limit because considerable hydrogen remained after the initial
11
12
13 dehydrogenation, and this remaining hydrogen could have continued to evolve during the
14
15
16
17 2nd dehydrogenation.
18
19
20
21
22

23 **Figure 2.** First and second cycle dehydrogenation of MgH₂/Sn with and without LiBH₄-
24
25
26 KBH₄ eutectic electrolyte. 1st cycle dehydrogenation (a, light red) with electrolyte; (b,
27
28 gray) without electrolyte. 2nd cycle dehydrogenation (c, dark red) with electrolyte; (d,
29
30
31 black) without electrolyte. (dashed curves) Corresponding temperatures, right axis.
32
33
34
35
36
37 Desorbed hydrogen (wt%) is with respect to the MgH₂/Sn mass only. Hydrogenation
38
39
40
41 treatment between cycles was conducted at 920 bar to 1000 bar while decreasing the
42
43
44 temperature from 215 °C to 175 °C, over 75 hr. Dehydrogenations were performed with
45
46
47 an initial hydrogen pressure of 2 bar H₂. The dehydrogenation temperature was limited
48
49
50
51 to 225 °C to avoid melting the Sn (T_m = 232 °C).
52
53
54
55
56
57
58
59
60

1
2
3
4 X-ray diffraction analysis confirmed that dehydrogenation indeed occurs, as shown in
5
6
7 Figures S4 and S5. Following dehydrogenation, Mg_2Sn was clearly seen as a crystalline
8
9
10 phase both with and without electrolyte. After subsequent hydrogen treatment with the
11
12
13 electrolyte, peaks for Mg_2Sn disappeared while those for MgH_2 and Sn grew, indicating
14
15
16 significant rehydrogenation. In contrast, without electrolyte, similar patterns were seen
17
18
19 before and after hydrogen treatment indicating that no or minimal reaction occurred.
20
21
22
23
24
25
26
27

28 *Electrolyte-assisted hydrogenation of MgB_2 .* Samples of milled MgB_2 with and without
29
30
31 electrolytes were treated in ~1000 bar hydrogen at 320 °C for 50 h (Figure S6). Two
32
33
34 electrolytes were evaluated. The first was the 0.725LiBH₄/0.275KBH₄ eutectic, the same
35
36
37 electrolyte used with the MgH_2 /Sn system described above. The second was a ternary
38
39
40 alkali metal iodide with the composition 0.33LiI/0.33KI/0.33CsI, which melts at ~210 °C
41
42
43 (Figure S7). To minimize any water content, this electrolyte was mixed and cycled to 300
44
45
46 °C several times prior to mixing with MgB_2 . All three samples were treated in hydrogen
47
48
49 simultaneously in a pressure vessel with multiple individual sample holders. Treatment
50
51
52 at 320 °C was chosen because previous work indicated only minor amounts of hydrogen
53
54
55
56
57
58
59
60

1
2
3 uptake (<~1 wt%) occurred at this temperature.³⁴ Subsequent dehydrogenations of the
4
5
6
7 hydrogen-treated samples are shown in Figure 3. Dehydrogenation of only ~0.3 wt% was
8
9
10 observed for the MgB_2 without electrolyte, indicating minimal hydrogen uptake, as
11
12
13 expected. In contrast, both samples with eutectic electrolytes showed significant
14
15
16 dehydrogenation of ~6 wt% H_2 (with respect to the mass of MgB_2). Thus, the presence
17
18
19 of liquid electrolyte increased the hydrogen uptake by ~20 \times , to ~40% of completion. The
20
21
22 initial rates at 250 °C to 300 °C for both eutectics were similar as seen by the similar
23
24
25 slopes at ~9 h and 20 h, respectively. However, the rate with the 0.33LiI/0.33KI/0.33CsI
26
27
28 eutectic decreased over time, ultimately requiring 350 °C to desorb ~6 wt% H_2 , while with
29
30
31 the 0.725LiBH₄/0.275KBH₄ eutectic, 6 wt% H_2 was desorbed at 300 °C. Two additional
32
33
34 samples with the 0.33LiI/0.33KI/0.33CsI eutectic, one with 31 wt% MgB_2 and another with
35
36
37 47 wt% MgB_2 (~1/2 the amount of eutectic), were similarly hydrogen treated but
38
39
40 dehydrogenated using a different apparatus in a different laboratory. The results, shown
41
42
43 in Figure S8, confirm those shown in Figure 3 and indicate that the improved hydrogen
44
45
46 uptake persists for lower electrolyte fractions.
47
48
49
50
51
52
53
54
55
56
57
58
59
60

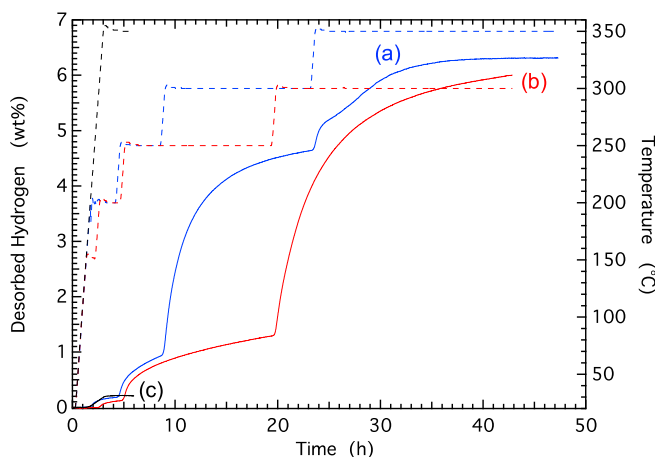


Figure 3. Dehydrogenation of MgB_2 following treatment in high pressure hydrogen with and without electrolytes. (a, blue) With 0.33LiI/0.33KI/0.33CsI eutectic, 31 wt% MgB_2 ; (b, red) with 0.725LiBH₄/0.275KBH₄ eutectic, 46 wt% MgB_2 ; (c, black) without electrolyte; (dashed curves) corresponding temperatures, right axis. The inflection in the rate of (a) at 25 h may be associated with slight foaming which was detected when removing the sample. Desorbed hydrogen (wt%) is with respect to the MgB_2 mass only. Dehydrogenation with 0.725LiBH₄/0.275KBH₄ eutectic was conducted into an initial pressure of 2 bar H₂; dehydrogenation with the 0.33LiI/0.33KI/0.33CsI eutectic was conducted into an initial vacuum.

1
2
3
4
5
6 The dehydrogenation results shown in Figure 3 are supported by ^{11}B NMR spectra
7
8
9 before and after hydrogen treatment as shown in Figure 4. For the MgB_2 without the
10
11
12 electrolyte, the ^{11}B NMR spectra before and after hydrogen treatment are nearly identical
13
14
15 (Figure 4a). A small peak at -41 ppm indicates $[\text{BH}_4]^-$ species with a fraction of ~3% of
16
17
18 the integrated ^{11}B signal area. In contrast, with the 0.33LiI/0.33KI/0.33CsI electrolyte after
19
20
21
22 hydrogen treatment (Figure 4b) there is a large signal at -39 ppm with an area of 71%,
23
24
25 while the area for MgB_2 decreases to 21%. There is also a small signal (4%) at -15 ppm
26
27
28 corresponding to $[\text{B}_{12}\text{H}_{12}]^{2-}$ species. There are small shoulders on the -39 ppm peak that
29
30
31 may indicate $[\text{BH}_4]^-$ species in different environments, possibly due to the presence of Li^+ ,
32
33
34
35
36
37
38 K^+ , and Cs^+ cations in the electrolyte.
39
40
41
42
43
44
45
46
47
48
49
50
51
52
53
54
55
56
57
58
59
60

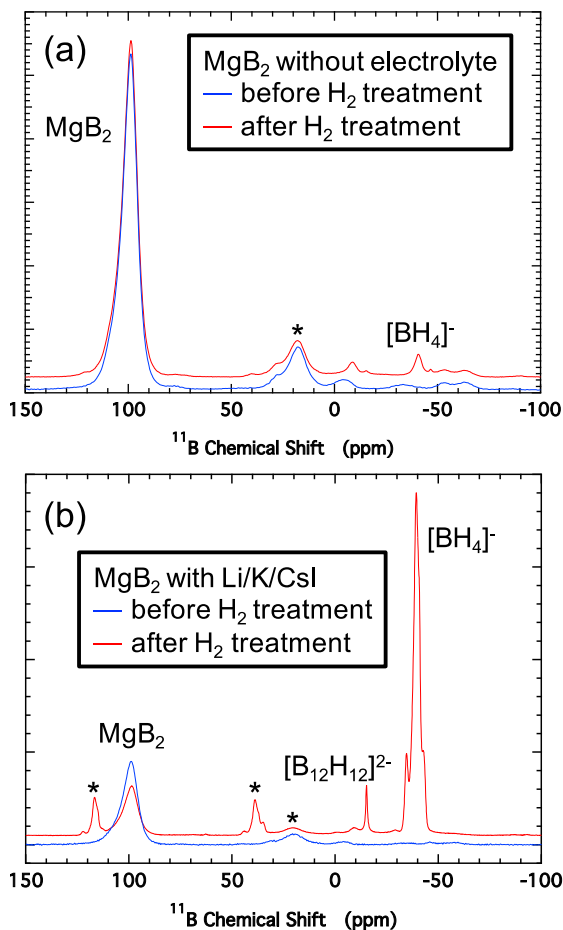
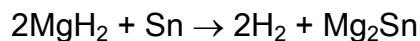


Figure 4. ^{11}B NMR spectra of MgB_2 with and without $0.33\text{LiI}/0.33\text{KI}/0.33\text{CsI}$ electrolyte before and after hydrogen treatment. (a) Without electrolyte, (blue) before hydrogen treatment, (red) after hydrogen treatment; (b) with $0.33\text{LiI}/0.33\text{KI}/0.33\text{CsI}$ electrolyte, (blue) before hydrogen treatment, (red) after hydrogen treatment. * indicates spinning sidebands.

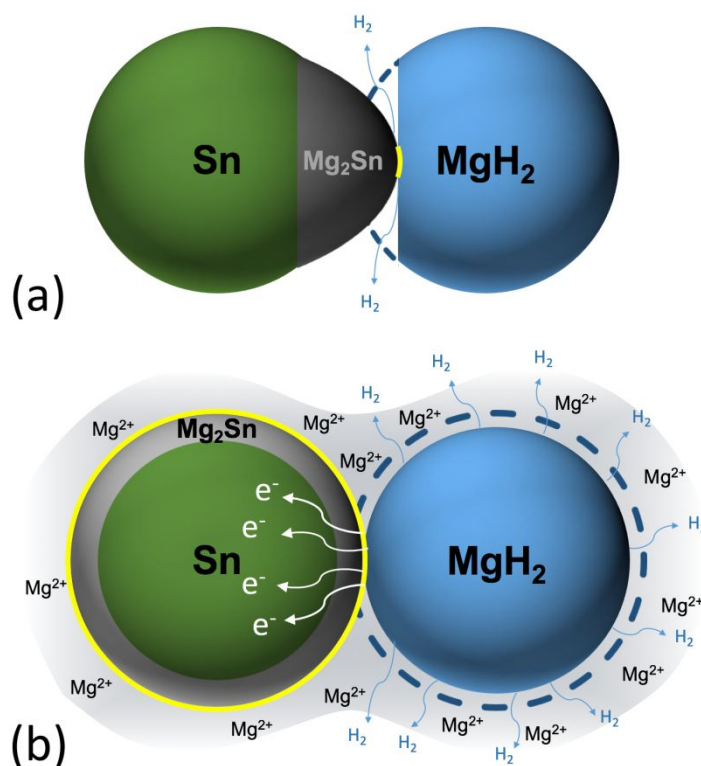
Discussion

Although the mechanisms of these reactions have not yet been studied in detail, the presented results demonstrate the efficacy of using electrolytes with hydride materials and reveals the importance of inter-particle transport in hydrogen exchange. For the MgH₂/Sn system, the overall reaction is given by



(1)

1
2
3
4 Dehydrogenation must involve concerted reaction between MgH_2 and Sn because Mg
5
6
7 metal, as a distinct phase, cannot form under the reaction conditions with the initial H_2
8
9
10
11 overpressure (ie, $P(\text{H}_2) \geq 2$ bar and $T_{\text{reaction}} \leq 225$ °C compared to $T_{\text{eq}}(2$ bar) ~ 300 °C).
12
13



38 Thus, Mg_2Sn can form only where MgH_2 and Sn are in direct contact at the atomic scale,
39
40
41 as depicted in Figure 5.
42
43
44
45
46
47

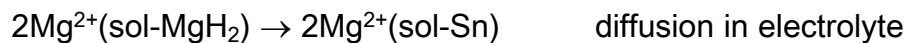
48 **Figure 5.** Dehydrogenation of MgH_2/Sn . (a) In the solid/solid reaction (without electrolyte)
49
50
51 formation of Mg_2Sn only occurs where MgH_2 and Sn are in contact at the atomic level
52
53
54
55 (shown in yellow). (b) In an electrolyte, solubilized Mg^{2+} ions can diffuse through the
56
57
58
59
60

1
2
3 electrolyte while electrons are conducted through solid-solid contacts enabling Mg_2Sn
4
5
6
7 formation over the whole surface of a Sn particle (shown in yellow).
8
9

10
11
12
13
14 However, MgH_2 at the surface of a magnesium hydride particle in contact with an
15
16
17 electrolyte could dissociate releasing H_2 and forming a Mg^{2+} ion and two electrons. The
18
19
20
21 Mg^{2+} ions could become solvated and diffuse in the electrolyte to the surface of a Sn
22
23
24 particle while the electrons are transported through solid-solid contacts. At the Sn particle
25
26
27 surface, $2\text{Mg}^{2+} + 4\text{e}^- + \text{Sn}$ can react to form Mg_2Sn . These steps are depicted in Figure
28
29
30
31 5 and given by
32
33



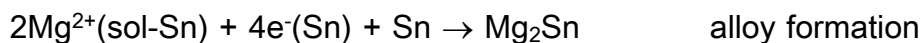
38 (2)
39
40



45 (3)
46
47



52 (4)
53
54
55
56
57
58
59
60



(5)

where $2\text{Mg}^{2+}(\text{sol-MgH}_2)$ and $2\text{Mg}^{2+}(\text{sol-Sn})$ refer to Mg^{2+} ions solubilized at the surfaces of MgH_2 and Sn, and $4\text{e}^{-}(\text{MgH}_2)$ and $4\text{e}^{-}(\text{Sn})$ refer to electrons in the MgH_2 and Sn solid phases, respectively. During diffusion (Eq. 3) the local environment of the $\text{Mg}^{2+}(\text{sol})$ is presumably modified from that of the Li^+ and K^+ cations in the molten $\text{LiBH}_4/\text{KBH}_4$ eutectic to account for the 2+ charge. Given the nature of the eutectic, it is unlikely that MgH_2 , a partially covalent hydride, or metallic Sn would be directly soluble. Although alloy formation (Eq. 5) may be initiated over the whole surface of the Sn that is wet by the electrolyte (Figure 5b), this step still involves solid state diffusion of Mg and/or Sn through the growing Mg_2Sn phase. Thus, this step may benefit from reduced particle sizes. The metallic nature of Sn may facilitate this reaction by enabling electron conduction (Eq. 4) from the MgH_2 (one reason that this system was chosen). Some support for this scenario, is provided by the increased dehydrogenation rates observed when MgI_2 was added to the $\text{LiBH}_4\text{-KBH}_4$ eutectic (Figure 1). Without any added Mg salt, there would theoretically be no Mg^{2+} ions to initiate the reaction, although we suspect that, in this case, oxidization

1
2
3 products (such as MgO or Mg(OH)₂) likely present at the surface of MgH₂ particles³⁵ could
4
5
6
7 provide some dissolved Mg²⁺ ions. With intentionally added MgI₂, the Mg²⁺ concentration
8
9
10 may well be increased enabling faster reaction. Although the solubility of MgI₂ in the
11
12
13 LiBH₄-KBH₄ eutectic is not known, iodide was chosen for its similar ionic size to [BH₄]⁻,
14
15
16
17 which should improve solubility.
18
19
20
21
22
23

24 For hydrogenation of MgB₂, hydrogen interacts, at least initially, with only a single
25
26
27 phase. Based on equilibrium phases, hydrogenation could proceed through a mixed
28
29
30 MgB₁₂H₁₂/MgH₂ step, although hydrogenation has been shown to proceed directly to
31
32
33
34 Mg(BH₄)₂ during the initial hydrogenation step.³⁶ In this case, similarly enhanced
35
36
37
38 transport of ionic species along the surface of MgB₂ particles could account for the
39
40
41
42 increased hydrogen uptake. For example, the possibility of localized Mg²⁺ or [BH₄]⁻
43
44
45 transport along the MgB₂/electrolyte interface could facilitate Mg(BH₄)₂ formation. In
46
47
48
49 addition, some dissolution of Mg(BH₄)₂ as it forms may expose fresh MgB₂ surfaces for
50
51
52
53 reaction. Even without atomic transport, the formation of Mg(BH₄)₂ from MgB₂ likely
54
55
56 involves significant increase in surface area, at least in part associated with the large
57
58
59
60

1
2
3
4 volume change of up to 400%. The free energy penalty associated with this increased
5
6
7 area may be lowered by the presence of solid-liquid electrolyte as opposed to solid-gas
8
9
10 interfacial energies.
11
12
13
14
15
16

17 These examples, MgH_2/Sn and MgB_2 , have been discussed as limiting cases of
18
19
20 enhanced inter-particle and particle surface transport. However, likely both inter-particle
21
22
23 and surface transport occur in both systems and can be facilitated by liquid electrolytes.
24
25
26
27 In contrast, we expect that solid state diffusion within particles would likely not be affected.
28
29
30

31 In addition to atomic transport, inclusion of electrolytes may enhance the reactivity of
32
33
34 solid phases by etching passivating surface layers. For example, specifically using the
35
36
37 iodide-based 0.33LiI/0.33KI/0.33CsI eutectic (or halide-based electrolytes in general)
38
39
40 may facilitate reaction by etching, or at least partially dissolving, surface oxides present
41
42
43 on the MgB_2 surface.³⁶ This dissolution would expose MgB_2 to hydrogen analogous to
44
45
46 the manner in which aqueous halide solutions are known to promote corrosion of metals,
47
48
49 such as aluminum, that have passivating oxides.³⁷
50
51
52
53
54
55
56
57
58
59
60

1
2
3
4 Ideally and most simply, an electrolyte would function only as a solvent for mobile ions
5
6
7 or passivating surface layers without further participating or altering the overall hydrogen
8
9
10 cycling reaction. However, to be suitable solvents for the hydride phase cations and be
11
12
13 compatible with the hydrogen chemical potentials required for hydrogen cycling, possible
14
15
16 electrolytes may likely need to be sufficiently chemically similar to the hydride phases that
17
18
19 they do alter or participate in the desired overall reaction. For example, for MgH_2/Sn with
20
21
22 the $\text{LiBH}_4\text{-KBH}_4$ electrolyte, Li_xSn alloys and $\text{Mg}(\text{BH}_4)_2$ are possible side reaction
23
24
25 products. For the initial characterization performed in this work, significant side reaction
26
27
28 was not observed. Specifically, the major phases observed by XRD after a single
29
30
31 dehydrogenation and rehydrogenation cycle were Mg_2Sn and $\text{MgH}_2 + \text{Sn}$, respectively
32
33
34 (Figure S4). Further work is needed to determine if side reaction products may
35
36
37 accumulate slowly over multiple cycles. We note that although side reactions may
38
39
40 ultimately occur, if meeting requirements, the overall hydride-electrolyte combination may
41
42
43
44
45
46
47
48
49 be considered as a suitable hydrogen storage material system.
50
51
52
53
54
55

56 Conclusion

1
2
3
4 In summary, we have used electrolytes to improve the hydrogen cycling in multiple-
5
6
7 phase hydrogen storage materials and shown significant improvements for the
8
9
10 dehydrogenation and rehydrogenation of MgH_2/Sn and the hydrogenation of MgB_2 .
11
12
13
14 These results clearly indicate that inter-particle transport between different phases and/or
15
16
17 transport over the surface of individual particles is an important aspect of the hydrogen
18
19
20 cycling reaction that can be facilitated (and studied) using electrolytes. The compositions
21
22
23 used in this study contained an excess of electrolyte (>50 wt% electrolyte mass fraction).
24
25
26
27 To be useful for practical hydrogen storage applications, lower electrolyte fractions (e.g.
28
29
30 <~25 wt%) would need to be demonstrated. We consider this a reasonable possibility
31
32
33
34 given that optimized modern Li-ion batteries contain ~15 wt% electrolyte with respect to
35
36
37 the full mass (active material + electrolyte mass). One path here is optimizing the particle
38
39
40 sizes. Larger particles have lower surface area and therefore require less electrolyte to
41
42
43 coat; however, they also have longer diffusion distances within and along particles.
44
45
46
47
48 Moving forward, a wide range of electrolytes may be considered including other eutectics,
49
50
51 solvents with dissolved salts, and ionic liquids, although thermal stability, chemical
52
53
54 stability at hydride chemical potentials, and vapor pressure all present stringent
55
56
57
58
59
60

1
2
3 requirements. Finally, it seems that the use of electrolytes could significantly improve the
4
5
6 rates of hydrogen exchange in perhaps many other complex hydride materials including
7
8
9
10 metal alanates, amides, borohydrides, and destabilized systems.
11
12
13
14
15
16
17

18 **Supporting information**

19
20
21
22 Experimental methods, other potential electrolytes investigated, tabular data from
23
24
25
26 Figure 1, Figures S1 to S8.
27
28
29

30 **Notes**

31
32
33
34
35 ** Current address: Phillips 66 Research Center, Bartlesville, OK 74003.
36
37

38 The authors declare no competing financial interests.
39
40
41
42
43
44
45
46
47
48

49 **Acknowledgments**

50
51
52
53
54
55
56
57
58
59
60

1
2
3
4 This work was supported by the U. S. Department of Energy under contract DE-
5
6
7 EE0007849. The NMR facility at the California Institute of Technology was supported by
8
9
10 the National Science Foundation (NSF) under Grant Number 9724240 and partially
11
12
13 supported by the MRSEC Program of the NSF under Award Number DMR-520565.
14
15
16 Sandia authors gratefully acknowledge research support from the U.S. Department of
17
18 Energy, Office of Energy Efficiency and Renewable Energy, Fuel Cell Technologies Office
19
20
21 through the Hydrogen Storage Materials Advanced Research Consortium (HyMARC).
22
23
24 Sandia National Laboratories is a multimission laboratory managed and operated by
25
26
27 National Technology and Engineering Solutions of Sandia, LLC., a wholly owned
28
29
30 subsidiary of Honeywell International, Inc., for the U.S. Department of Energy's National
31
32
33 Nuclear Security Administration under contract DE-NA-0003525. This paper describes
34
35
36 objective technical results and analysis. Any subjective views or opinions that might be
37
38
39 expressed in the paper do not necessarily represent the views of the U.S. Department of
40
41
42 Energy or the United States Government.
43
44
45
46
47
48
49
50
51
52
53
54
55
56
57
58
59
60

1
2
3
4
5
6
7
8
9
10
11 **References**
12

13
14 (1) Li, H.-W.; Wu, G.; Chen, P. Solid Hydrogen Storage Materials: Non-interstitial
15
16
17 Hydrides, Chap 15 in *Hydrogen Energy Engineering* Sasaki, K.; Li, H.-W.; Hayashi, A.;
18
19
20 Yamabe, J.; Ogura, T.; Lyth, S. M. Eds., **2016**, Springer Japan.

21
22
23
24
25 (2) Callini, E.; Atakli, Z. O. K.; Hauback, B. C.; Orimo, S.; Jensen, C.; Dornheim, M.;
26
27
28 Grant, D.; Cho, Y. W.; Chen, P.; Hjörvarsson, B.; et al. Complex and Liquid Hydrides for
29
30
31 Energy Storage. *Appl. Phys. A* **2016**, *122*:353.

32
33
34
35
36 (3) Stavila, V.; Klebanoff, L.; Vajo, J. J.; Chen, P. Development of On-Board Reversible
37
38
39 Complex Metal Hydrides for Hydrogen Storage, Chap. 6 in *Hydrogen Storage Technology*
40
41
42 *Materials and Applications* Klebanoff, L. ed., **2013**, CRC Press.

43
44
45
46
47 (4) Vajo, J. J.; Olson, G. L. Hydrogen Storage in Destabilized Chemical Systems. *Scr.*
48
49
50
51 *Mater.* **2007**, *56*, 829– 834.
52
53
54
55
56
57
58
59
60

1
2
3
4 (5)
5
6

7 Dornheim, M.; Doppiu, S.; Barkhordarian, G.; Bösenberg, U.; Klassen, T.; Gutfleisch, O.
8
9
10 ; Bormann, R. Hydrogen Storage in Magnesium-Based Hydrides and Hydride
11
12 Composites. *Scr. Mater.* **2007**, *56*, 841– 846.
13
14
15
16
17

18 (6) Frankcombe, F.; Proposed Mechanisms for the Catalytic Activity of Ti in NaAlH₄.
19
20
21
22 *Chem. Rev.* **2012**, *112*, 2164-2178.
23
24
25

26 (7) Yu, X.; Tang, Z.; Sun, D.; Ouyang, L.; Zhu, M. Recent Advances and Remaining
27
28 Challenges of Nanostructured Materials for Hydrogen Storage Applications. *Prog. Mater.*
29
30
31
32 *Sci.* **2017**, *88*, 1-48.
33
34
35
36

37 (8) de Jongh, P. E.; Allendorf, M.; Vajo, J. J.; Zlotea, C. Nanoconfined Light Metal
38
39
40
41
42
43
44
45
46
47
48
49
50
51
52
53
54
55
56
57
58
59
60
Hydrides for Reversible Hydrogen Storage. *MRS Bull.* **2013**, *38*, 488– 494.

59 (9) Vajo, J. J. Influence of Nano-Confinement on the Thermodynamics and
60
Dehydrogenation Kinetics of Metal Hydrides. *Curr. Opin. Sol. State Mater, Sci.* **2011**, *15*,
52-61.

1
2
3
4 (10) Zheng, X.; Xu, W.; Xiong, Z.; Chua, Y.; Wu, G.; Qin, S.; Chen, H.; Chen, P. Ambient
5
6
7 Temperature Hydrogen Desorption from $\text{LiAlH}_4\text{-LiNH}_2$ Mediated by HMPA. *J. Mater.*
8
9
10 *Chem.* **2009**, *19*, 8426-8431.

11
12
13
14 (11) Zheng, X.; Xiong, Z.; Qin, S.; Chua, Y.; Chen, H.; Chen, P. Dehydrogenation of
15
16
17 LiAlH_4 in HMPA. *Int. J. Hy. Energy* **2008**, *33*, 3346-3350.

18
19
20
21
22 (12) Xiong, Z.; Chua, Y.-S.; Wu, G.; Xu, W.; Chen, P.; Shaw, W.; Karamkar, A.; Linehan,
23
24
25 J. Smurthwaite, T.; Autrey, T. Interaction of Lithium Hydride and Ammonia Borane in THF.
26
27
28 *Chem. Comm.* **2008**, 5595-5597.

29
30
31
32
33 (13) Zhang, S.; Taniguchi, A.; Xu, Q.; Takeichi, N. Takeshita, H. T.; Kuriyama, N.;
34
35
36 Kiyobayashi, T.; Understanding the Effect of Titanium Species on the Decomposition of
37
38
39 Alanates in Homogeneous Solution. *J. Alloy. Compds.* **2006**, *413*, 218-221.

40
41
42
43
44 (14) Mohtadi, R.; Sivasubramanian, P.; Hydrogen Release from Complex Metal
45
46
47
48 Hydrides by Solvation in Ionic Liquids. **2014**, US patent 8,771,635.

1
2
3
4 (15) Humphries, T. D.; Birkmire, D.; McGrady, G. S.; Hauback, B.; Jensen, C. M.;
5
6
7 Regeneration of LiAlH₄ at Sub-Ambient Temperatures Studied by Multinuclear NMR
8
9
10 Spectroscopy. *J. Alloy. Compds.* **2017**, *723*, 1150-1154.
11
12

13
14 (16) Chong, M.; Matsuo, M.; Orimo, S.; Autrey, T.; Jensen, C. M.; Selective Reversible
15
16
17 Hydrogenation of Mg(B₃H₈)₂/MgH₂ to Mg(BH₄)₂: Pathway to Reversible Borane-Based
18
19
20
21 Hydrogen Storage? *Inorg. Chem.* **2015**, *54*, 4120-4125.
22
23

24
25 (17) Ni, C.; L. Yang, Muckerman, J. T.; Graetz, J.; Aluminum Hydride Separation using
26
27
28
29 N -Alkylmorpholine. *J. Phys. Chem. C* **2013**, *117* 14983.
30
31

32
33 (18) Graetz, J.; Wegrzyn, J.; Reilly, J. J. Regeneration of Lithium Aluminum Hydride
34
35
36
37 (LiAlH₄). *J. Amer. Chem. Soc.* **2008**, *130*, 17790.
38
39

40
41 (19) Wang. J.; Ebner. A. D.; Ritter, J. A.; Synthesis of Metal Complex Hydrides for
42
43
44
45 hydrogen Storage. *J. Phys. Chem. C* **2007**, *111*, 14917-14924.
46
47

1
2
3
4 (20) Wang, J.; Ebner, A. D.; Ritter, J. A.; Physiochemical Pathway for Cyclic
5
6
7 Dehydrogenation and Rehydrogenation of LiAlH_4 . *J. Am. Chem. Soc.* **2006**, *128*, 5949-
8
9
10 5954.

11
12
13
14 (21) Wang, H.; Wu, G.; Cao, H.; Pistidda, C.; Chaudhary A.-L.; Garroni, S.; Dornheim,
15
16
17 M.; Chen, P. Near Ambient Condition Hydrogen Storage in a Synergized Tricomponent
18
19
20
21 Hydride System. *Adv. Energy Mater.* **2017**, 1602456.

22
23
24
25 (22) Tan, Y.; Guo, Y.; Li, S. Sun, W.; Zhu, Y.; Li, Q.; Yu, X.; A liquid-Based Eutectic
26
27
28
29 System: $\text{LiBH}_4 \cdot \text{NH}_3 - n\text{NH}_3\text{BH}_3$ with High Dehydrogenation Capacity at Moderate
30
31
32
33 Temperature. *J. Mater. Chem.* **2011**, *21*, 14509-14515.

34
35
36
37 (23) Graham, K. R.; Kemmitt, T.; Bowden, M. E.; High Capacity Hydrogen Storage in a
38
39
40
41 Hybrid Ammonia Borane-Lithium Amide Material. *Energy Environ. Sci.* **2009**, *2*, 706-710.

42
43
44
45 (24) Crivello, J.-C.; Denys, R. V.; Dornheim, M.; Felderhoff, M.; Grant, D. M.; Huot, J.;
46
47
48
49 Jensen, T. R.; de Jongh, P.; Latroche, M.; Walker, et al.; V. A. Mg-Based Compounds for
50
51
52
53 Hydrogen and Energy Storage. *Appl. Phys. A* **2016**, *122*:85.

1
2
3 (25) Chaudhary, A.-L.; Paskevicius, M.; Sheppard, D. A.; Buckley, C. E.;
4
5
6
7 Thermodynamic Destabilization of MgH₂ and NaMgH₃ using Group IV Elements Si, Ge,
8
9
10 or Sn. *J. Alloys Compd.* **2015**, *623*, 109-116.
11
12

13
14 (26) Janot, R.; Cuevas, F.; Latroch, M. Percheron-Guégan, A.; Influence of Crystallinity
15
16
17 on the Structural and Hydrogenation Properties of Mg₂X Phases (X = Ni, Si, Ge, Sn).
18
19
20
21 *Intermetallics* **2006**, *14*, 163-169.
22
23

24
25 (27) Chaudhary, A.-L.; Sheppard, D. A.; Paskevicius, M; Webb, C. J.; Gray, E. M.
26
27
28 Buckley, C. E. Mg₂Si Nanoparticle Synthesis for High Pressure Hydrogenation. *J. Phys*
29
30
31
32
33 *Chem. C* **2014**, *118*, 1240-1247.
34
35

36
37 (28) Polanski, M.; Bystrzycki, J.; The Influence of Different Additives on the Solid-State
38
39
40 Reaction of Magnesium Hydride (MgH₂) with Si. *Int. J. Hydrog. Energy* **2009**, *34*, 7692-
41
42
43
44 7699.
45
46

47
48 (29) Vajo, J. J.; Mertens, F.; Ahn, C. C.; Bowman Jr., R. C.; Fultz, B.; Altering Hydrogen
49
50
51 Storage Properties by Hydride Destabilization through Alloy Formation: LiH and MgH₂
52
53
54
55 Destabilized with Si. *J. Phys. Chem. B* **2004**, *108*, 13977-13983.
56
57

1
2
3 (30) Zavorotynska, O.; El-Karbach, A.; Deledda, S. Hauback, B. Recent Progress in
4 Magnesium Borohydride $Mg(BH_4)_2$: Fundamentals and Applications for Energy Storage.
5
6
7
8
9
10 *Int. J. Hydrog. Energy* **2016**, *41*, 14387-14403.

11
12
13
14 (31) Allendorf, M. D.; Stavila, V.; White, J. L.; Wang, T. C.; He, Y.; Klebanoff, L. E.;
15 Kolasinski, R. D.; El Gabaly, F. Zhao, X. HyMARC: Sandia's Technical Effort. *Hydrogen*
16
17
18
19
20
21
22 *and Fuel Cells Program 2018 Annual Merit Review and Peer Evaluation. 2018*
23
24
25 https://www.hydrogen.energy.gov/pdfs/review18/st128_allendorf_2018_o.pdf.

26
27
28
29 (32) Severa, G.; Rönnebro, E.; Jensen, C. M. Direct Hydrogenation of Magnesium
30 Boride to Magnesium Borohydride. *Chem Commun.* **2010**, *46*, 421-423.

31
32
33 (33) Ley, M. B.; Roedern, E.; Jensen, T. R.; Eutectic Melting of $LiBH_4$ - KBH_4 . *Phys.*
34
35
36
37
38
39
40
41 *Chem. Chem. Phys.* **2014**, *16*, 24194-24199.

42
43
44 (34) Newhouse, R. J. Part I. Femtosecond Transient Absorption Studies of Metal and
45
46
47
48
49
50
51
52
53
54
55
56
57
58
59
60
Hydride Materials for Hydrogen Storage Applications. Ph.D. Dissertation, University of
California Santa Cruz, Santa Cruz, CA, 2011.

1
2
3 (35) House, S. D.; Vajo, J. J.; Ren, C.; Zaluzec, N. J.; Rockett, A. A.; Robertson, I. M.;
4
5
6
7 Impact of Initial Catalyst Form on the 3D Structure and Performance of Ball-Milled Ni-
8
9
10 Catalyzed MgH₂ for Hydrogen Storage. *Int. J. Hydrog. Energy* **2017**, *42*, 5177-5187.

11
12
13
14 (36) Ray, K. G.; Klebanoff, L. E.; Lee, J. R. I.; Stavila, V.; Heo, T. W.; Shea, P.; Baker,
15
16
17
18 A. A.; Kang, S.; Bagge-Hansen, M.; Liu, Y.-S.; et al.; Elucidating the Mechanism of MgB₂
19
20
21 Initial Hydrogenation *via* a Combined Experimental-Theoretical Study. *Phys. Chem.*
22
23
24
25 *Chem. Phys.* **2017**, *19*, 22646.

26
27
28
29 (37) Natishan, P. M.; O'Grady, W. E. Chloride Ion Interactions with Oxide-Covered
30
31
32
33 Aluminum Leading to Pitting Corrosion: A Review. *J. Electrochem. Soc.* **2014**, *161*, C421-
34
35
36
37 C432.

TOC Graphic

